Utilization of Deterministic Transport Methods for Analysis of Pebble Bed Reactors

Bismark Tyobeka[1], Kostadin Ivanov*[1] and Andreas Pautz[2]
[1] *The Pennsylvania State University, Nuclear Engineering Program, University Park, State College, PA, 16802, USA*
[2] *Erlangen, Germany*

Abstract

This paper presents an overview of the investigations on the need for deterministic transport methods for the analysis of pebble-bed reactors. To account for the transport effects present in the PBMR design that cannot be modeled accurately with the diffusion theory, a two-dimensional neutronics solver based on transport theory is implemented in the Penn State NEM-THERMIX code system. The necessity of equipping neutronics analysis codes with neutron transport theory capability is investigated along with the challenges to accomplish this in an efficient and versatile manner. For this purpose a time-dependent version of the two-dimensional neutron transport code DORT is utilized as a first step. The developed benchmark test cases, based on the PBMR 268 MW design, are used for this work, and results from the comparative analyses of these test cases are presented. The results show clearly that even in steady-state calculations, the differences between diffusion and transport-based methods in analyzing the PBMR are observed and need to be addressed.

KEYWORDS: PBMR, NEM, DORT, neutronics, control rods, diffusion, transport

1. Introduction

The diffusion theory model is currently being used as a routine tool to analyze most of the nuclear reactor design problems. In spite of its limitations, for most applications so far the diffusion theory provides adequate performance (in terms of optimal combination of accuracy and efficiency), and when it fails to deliver the necessary accuracy, for licensing purposes for example, the transport theory is deployed on a limited basis. Three features of the Pebble Bed Modular Reactor (PBMR), in particular, demand transport theory modeling:

a) The presence of the void at the top of the pebble-bed;
b) The asymmetric arrangement of the control rods in the side reflectors;
c) The heterogeneous nature of the core, surrounded by multiple layers of graphite.

The work performed here has been divided into two parts. The first one was to identify the transport effects in the PBMR design and for this purpose, the DORT transport code was used [1]. The underlying justification for this choice is because as part of these studies we are envisioning coupling DORT with THERMIX-DIREKT [2] in the NEM-THERMIX [3] coupled code environment. In the second part of this study, PBMR 268 MW three-dimensional (3-D) models for MCNP and TORT are

* Corresponding Author

developed in order to further evaluate 3-D related transport effects, in this case control rod modeling.

2. Development of Two-dimensional PBMR Core S_N Model

In order to make a case for the need of using advanced deterministic transport methods for both steady-state and transient analysis of high temperature reactors of pebble-bed type, a transport model of the PBMR core was developed using the DORT code. The version of DORT used in this work is the DORT/DORT-TD code from the Technical University of Munich, Germany [4]. In this system, DORT-TD serves as a pre-processor for DORT input generation and then the calculations are performed by DORT. It was essential to also perform diffusion calculations for comparison, and the Penn State NEM code was used for this purpose. The following summarizes the main features of DORT/ DORT-TD:

a) Arbitrary quadrature S_N-order,
b) Arbitrary scattering P_N order of cross-sections;
c) Arbitrary number of energy groups;
d) Two-dimensional (2-D) geometry options available: x-y, r-θ, and r-z ;
e) Solution algorithm based on the usual inner-outer iteration scheme;
f) Acceleration of inner iterations by the Coarse-Mesh-Rebalance method (CMR).

The main features of the NEM code, developed at the Pennsylvania State University (PSU), are summarized as follows:

a) 3-D multi-group nodal diffusion code ;
b) Models both steady state and transient core conditions based on the Nodal Expansion Method (NEM);
c) Solves the nodal equations in three dimensions using the transverse integration procedure and is based on the partial current formulation of the nodal balance equations;
d) Have options for modeling of 3-D Cartesian, cylindrical and hexagonal geometries.

2.1 Benchmark Test Cases

The PBMR 268 MW benchmark specification [5] provides the basis for this work. The reference design for this benchmark problem is derived from the 268 MW PBMR design. Several simplifications were made to the design in this specification in order to limit the need for any further approximations to a minimum. The simplifications make the core design essentially two-dimensional (r-z) – see Figure 1. It includes flattening of the pebble bed's upper surface and the removal of the bottom cone and de-fuel channel that results in a flat bottom reflector. Flow channels within the pebble bed have been simplified to be parallel and at equal speed while the dynamic central column and mixing zone widths were defined to be constant over the total axial height. The control rods in the side reflector are modeled as a cylindrical skirt (also referred to as a grey curtain) with a given B-10 concentration.

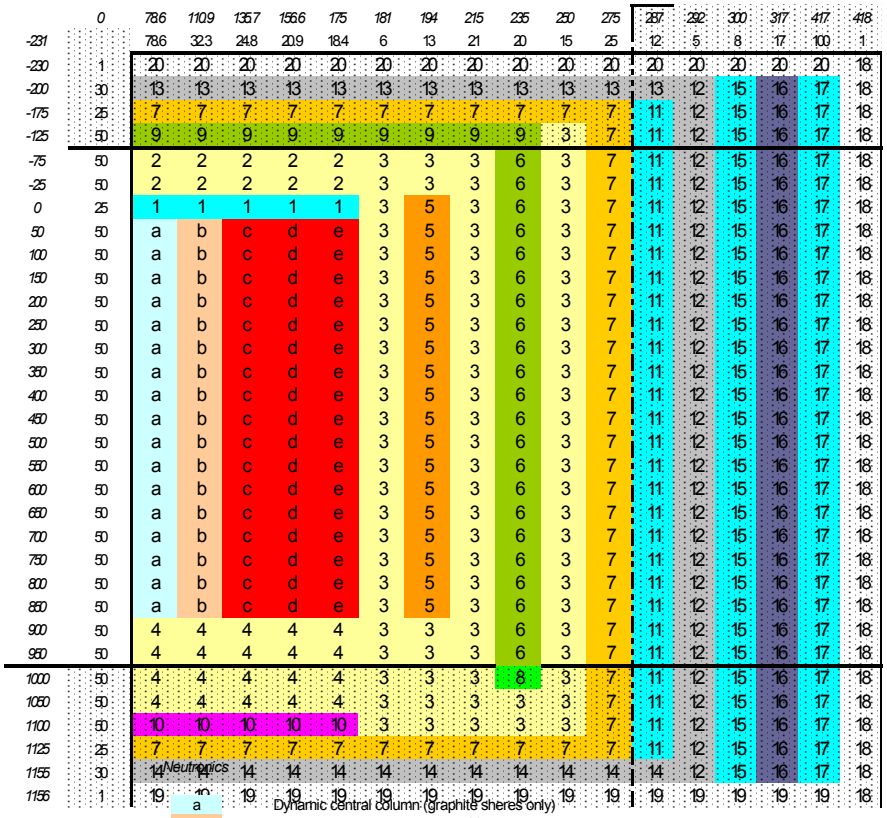

Figure 1. PBMR 268 MW Core Layout and Material Identification

The modeled test cases are variations of Case N2 in the benchmark specification. Case N2 is the equilibrium core of the PBMR but with fewer isotopes (some fission products excluded). In this work, the utilized cross sections were generated with the MICROX-2 code [6]. Initially, seven groups were generated for the transport calculations (DORT and TORT) and then for the diffusion calculations (NEM), these seven groups were collapsed to two groups. Up-scattering is also treated in MICROX-2 and hence modeled in DORT and TORT calculations. The first calculations performed involve a PBMR 268 MW Case N2 as described in [5] but with the control rods fully inserted and in the second set of calculations, the control rods were either withdrawn or partially inserted. In both calculation sets, the effect of the void at the top of the pebble-bed is investigated by modeling it as a layer of helium, and in another instance, by simply replacing it with a layer of graphite. Calculations were performed for 900K temperature conditions, i.e. cross sections were generated at this temperature.

3. Results for Two-dimensional Transport Effects.

The obtained results show a very interesting comparison between NEM and DORT, which are two codes using different methodologies. The first observation is from Table 1 that at the level of integral parameters such as k_{eff}, there is a very good agreement between NEM and DORT when the void is not modeled (73 pcm). The introduction of the void makes the difference much larger (364 pcm).

Table 1: Case N2 - Control Rods Fully Inserted

	With the void region modeled			Void replaced by graphite		
	k_{eff} value			k_{eff} value		
	NEM	DORT	Difference dk/k(pcm)	NEM	DORT	Difference dk/k(pcm)
900K	0.92411	0.92076	-364	0.92413	0.92481	+73

When one compares the normalized core average axial power distribution for Case N2 as a representative case, where spatial effects should be more pronounced, one notices that the void causes a power curve shift as shown in Figure 2. Obviously, the diffusion theory incorrectly predicts the fluxes and hence the power around the void region and this results in a power curve shift that is observed.

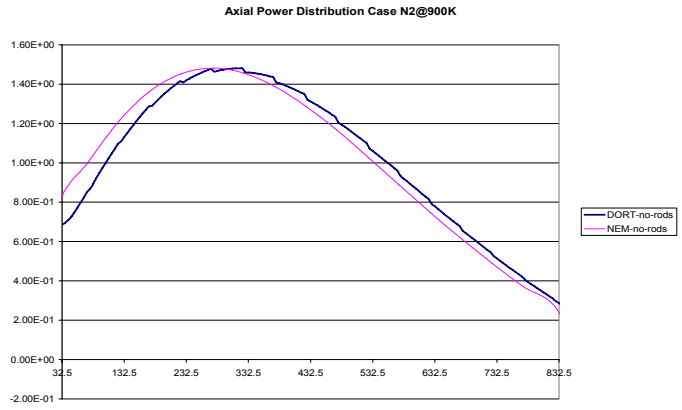

Figure 2: Axial Power Distribution for Case N2 (Void Sensitivity Studies)

4. Parametric Studies

The accuracy of a S_N calculation is impacted by spatial discretization, angular quadrature order, scattering order and energy group structure. To optimize the model in terms of accuracy and efficiency, parametric studies were carried out on these four parameters.

4.1 Studies on Angular Quadrature Order and Cross-section Scattering Order

With 29025 spatial meshes in 2-D cylindrical geometry (135(r), 215(z)) and 7-energy group cross sections, eight different combinations of fully symmetric quadrature orders and cross-section scattering orders were utilized in separate calculations, namely, P_1S_2, P_1S_4, P_1S_6, P_3S_8, P_3S_{10}, P_3S_{12}, P_3S_{14} and P_3S_{16}. The results of the study are as shown in Table 2 and Figure 3.

Table 2: k_{eff} Results of Studies on Angular Quadrature and Scattering Order

Order	k_{eff}	Difference (pcm)
P_1S_2	1.05817	-41 pcm
P_1S_4	1.05859	2 pcm
P_1S_6	1.05862	-1 pcm
P_3S_8	1.05861	0 pcm
P_3S_{10}	1.05861	0 pcm
P_3S_{12}	1.05860	1 pcm
P_3S_{14}	1.05863	-2 pcm
P_3S_{16} (reference)	1.05861	n/a
NEM	1.06017	-147 pcm

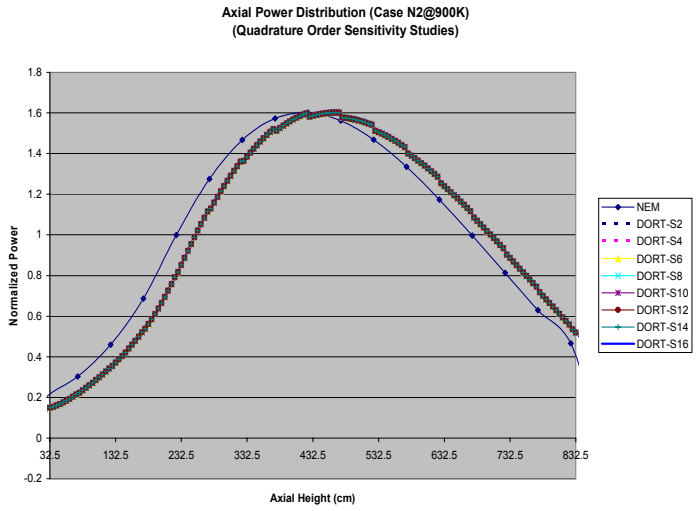

Figure 3: Axial Power Distribution for Case N2 (Studies on Quadrature Order)

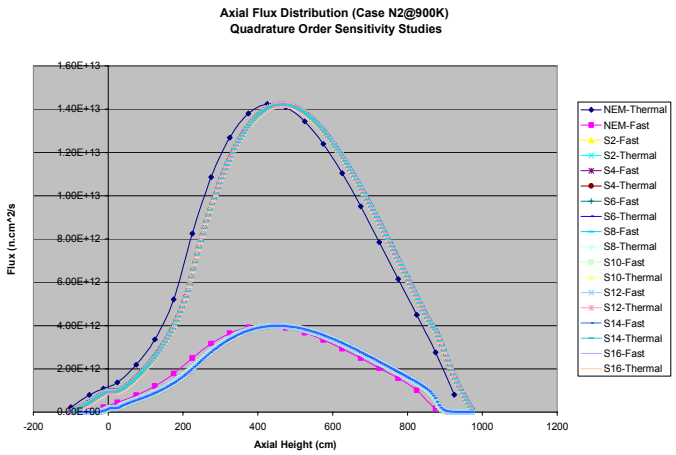

Figure 4: Axial Group Flux Distribution for Case N2 (Studies on Quadrature Order)

From the results shown in Figure 3, Figure 4 and Table 2, it can be seen that the eigenvalue, axial power and flux distributions in DORT (seven energy groups) change very slightly as the result of varying angular quadrature and scattering order, especially after S_4. This is important because the higher the angular quadrature order, the longer the inner iteration sweeps will take, and therefore resulting in long computational times. For comparison purposes, the NEM results (in two groups) were also included in the figures and table, and there is a visible shift between NEM and DORT fluxes and powers. The eigenvalue compares reasonably well between transport and diffusion calculations for this case.

4.2 Studies on spatial discretization/nodalization

With the P_1S_4 quadrature and scattering orders, four variations from the base case, consisting in total of 29025 meshes, were considered in this study namely:

- Axial discretization only (halving the number of nodes for each region in the axial direction)
- Radial discretization only (halving the number of nodes for each region in the radial direction)
- Both axial and radial discretization (halving the both the axial and radial nodes)
- Both axial and radial discretization (doubling the number of nodes in both axial and radial directions

The results for these cases are summarized in Table 3 where the difference in pcm is calculated in regard to the base case.

Table 3: k_{eff} Results for Case N2 (Studies on Spatial Discretization)

NODALIZATION	k_{eff}	Diff. (pcm)	CASE
29025 meshes (135(r), 215(z))	1.05860	n/a	base
14512.5 meshes, 135 (r), 107.5 (z)	1.05860	0	½ axial
14512.5 meshes 67.5 (r), 215 (z)	1.05860	0	½ radial
7256.25 meshes 67.5 (r) 107.5 (z)	1.05860	0	½ both
58050 meshes 270 (r), 450(z)	1.05863	-3	Double both

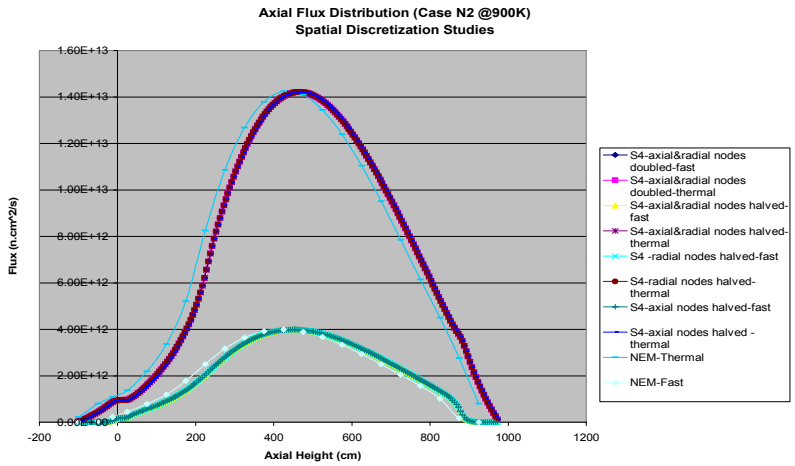

Figure 5: Axial Group Flux Distribution for Case N2 (Studies on Spatial Discretization)

From the results shown in Table 3 and Figure 5 it can be seen that eigenvalue, and fluxes in DORT are not affected much by the change in spatial discretization for this benchmark problem. This fact indicates that even coarser mesh can yield accurate results and thereby reducing the computational time. However, the shift in the powers and fluxes between NEM and DORT still remains.

4.3 Studies on energy group structure

DORT calculations were performed with three different energy group numbers namely: 4 groups, 7 groups and 13 groups with control rods fully inserted. The boundaries (cut-off points) for these group structures are as follows respectively: 1.000E+07 1.11090E+05 2.90232E+01 2.38237E+00 0.00 (eV) for the 4 group structure, 1.000E+07 1.11090E+05 7.1017400E+03 2.90232E+01 2.38237E+00 1.85539E+00 0.0 (eV) for the 7 group structure, and 1.000E+07 3.678E+06 1.11090E+05 7.1017400E+03 130.07 2.90232E+01 8.3153 2.38237E+00 1.85539E+00 0.625 0.200 0.075 0.0 (eV) for the 13 group structure. The selection of these group structures was motivated by both describing correctly the physical phenomena (physics) involved, and experience gained from the THTR and AVR research reactors. Performing group sensitivity studies is a necessary exercise because in transient studies using a large number of energy groups for a coupled code makes the calculation almost impossible due to high computational costs. The obtained results are shown in Table 4 and Figure 6.

Table 4: k_{eff} Results for Case N2 (Studies on Energy Group Structure)

CASE	k_{eff} (Rods partially inserted)	k_{eff} (Rods fully inserted)	Differential CRW (pcm/cm)
4 - energy groups	1.058310	0.922449	19.75
7 – energy groups	1.058538	0.920801	20.02
13 – energy groups	1.059697	0.917085	20.70

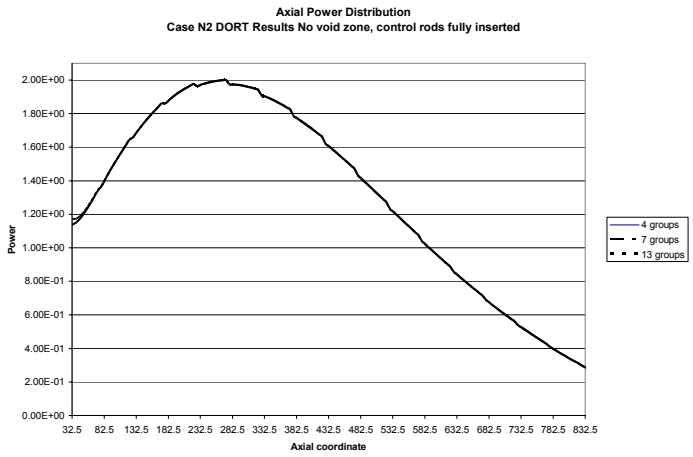

Figure 6: Axial Power Distribution for Case N2 (Studies on Energy Group Structure)

From the Table 4 and Figure 6 two things can be observed, namely, that for the eigenvalue, there is a significant change as one increases the number of energy groups. The overall difference of 5% is observed in the differential control rod worth between 4 groups and 13 groups. The trend seems to be that as one increases the number of energy groups, this difference may increase but this will be investigated later in the study. However, for the power distribution, the differences are quite small, except at the edges of the core, where there are slightly increased differences due to the treatment of the graphite reflector in different energy groups, i.e. for 13 energy group there is a better treatment of the scattering properties of graphite at the edges of the core (reflector regions), hence the small peak, which is due to the neutrons "pile-up" as they are scattered back into the core.

4.4 Conclusions Drawn from Parametric Studies.

From the results of the parametric studies shown above, one can draw the following conclusions:

a) Very little change in the eigenvalue, fluxes and power for DORT as one changes the quadrature order, especially after S_4. Using P_1S_4 as the representative quadrature for this problem is a reasonable approximation;
b) There are also very small effects on power shape, fluxes and eigenvalues due to spatial discretization;
c) There is very little effect on the powers and 5% difference in control rod worths between 4 groups and 13 groups. These differences can be tolerated for now and will be investigated later when the need arises;
d) There is a shift in both group flux and power distributions between NEM and DORT for all parametric studies carried out. This is the subject of the next section.

5. Evaluation of 2-D PBMR Transport Effects

In order to investigate the two-dimensional transport effects in the PBMR, studies were performed to isolate different effects. The first study was to investigate the effects of void cavity at the top of the pebble-bed by modeling cases with and without this feature. The second study was to investigate the effect of control rods by modeling cases with control rods partially inserted and fully inserted. For cases where the void region was excluded, the material composition of this region was replaced with a layer of graphite. All these studies were performed with P_1S_4 angular quadrature, 7-energy groups and 29025 meshes (135(r), 215(z)). Calculations were performed at 900K temperature conditions, and the results are provided in Figures 7 through 10.

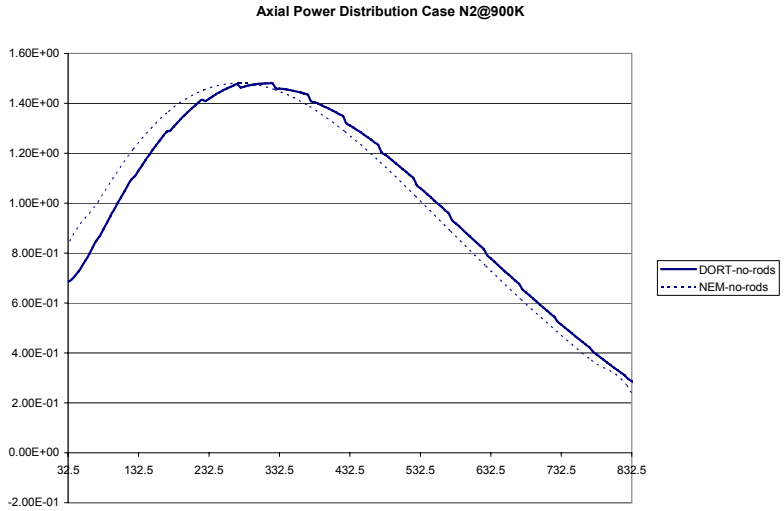

Figure 7: Axial Power Distribution for Case N2 (Studies on Void and Control Rod Effects)

From Figure 7 it is observed that removing the rods does not address the shift in the power distribution between transport and diffusion theory results. Note that the NEM calculations were performed with a rather coarser mesh, since it is expected that nodal methods should still yield accurate results even with coarse mesh. Subsequently this mesh was refined, to make sure that the shift does not come from mesh effects. In this way, the central graphite column (originally 78.63 cm) was divided into four nodes of 19.65 cm radially; the same was done for the mixing zone, the fuel regions and the graphite side reflector. The calculations were done with control rods fully inserted and fully withdrawn, to also investigate if the shift has anything to do with control rods. For both these instances, the void was modeled, i.e. as a layer of helium and not replaced with a graphite layer. The results are shown in Figures 8 and 9.

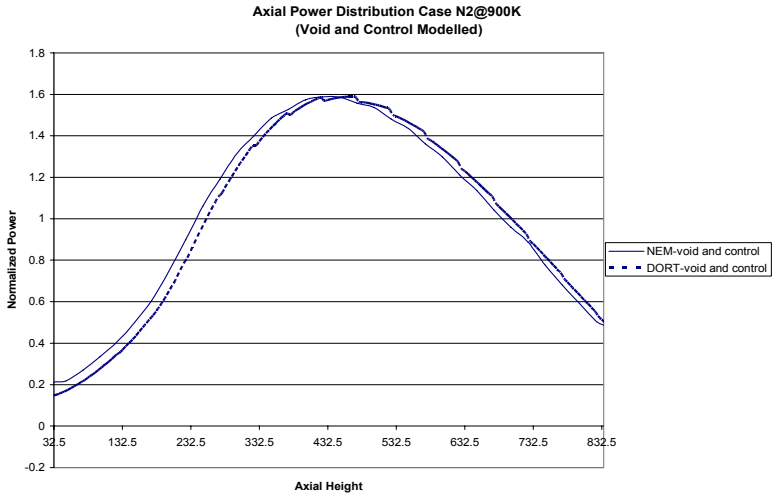

Figure 8 : Axial Power Distribution for Case N2 (Studies on Control and Void Effects)

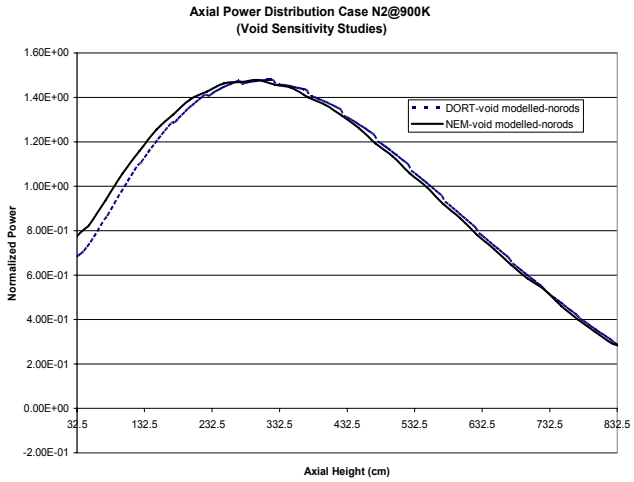

Figure 9: Axial Power Distribution for Case N2 (Studies on Control and Void Effects)

As confirmed by the results it appears that mesh effects played a significant role in the power shift between DORT and NEM. However, even with finer mesh in nodal diffusion, the presence of the void causes a shifting in the power. At this point, control rods can also be eliminated as the cause of this shift because as seen in Figures 8 and 9, the shift still remains regardless of the presence or absence of control rods. When control rod and the void are completely eliminated from the model, there is an excellent agreement between diffusion and transport theory results as shown in Figure 10.

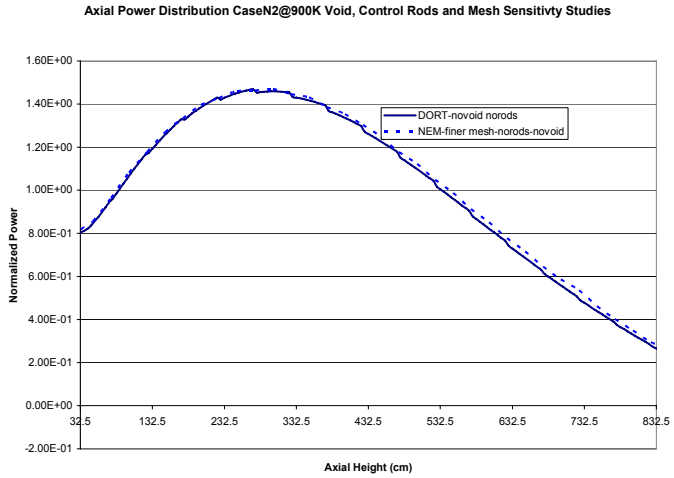

Figure 10: Axial Power Distribution for Case N2 (Studies on Control and Void Effects)

In Figure 10 where a fine mesh nodal diffusion method (NEM) is compared with transport (DORT), the power at the top of the core, where the void region would normally be, is observed to have been over-predicted by diffusion theory. In the void region, the only material present is helium gas, which is a rather transparent gas, and hence no interactions are expected. Neutron streaming causes the leakage out of the system at this region to be higher. One would therefore expect the flux to be just about flat or decreasing, hence the power curve is expected to be as predicted by DORT at the void region. Diffusion theory on the other hand over-predicts the flux (and hence the power) suggesting that some phenomena is taking place in this region, which is a misrepresentation. This effect can be more pronounced during

transients as peak power occurrence can be wrongly predicted in diffusion theory. This justifies the development of a coupled neutronics-thermal hydraulics transport theory-based code system, which can be used to provide reference solutions for benchmarks and to investigate the transport effects present in the PBMR design. As mentioned in the introduction, another transport effect in the PBMR core is the presence of control rods in the side reflector, where three-dimensional modeling is necessary. In the preceding investigations, the control rods were approximated as a cylindrical grey curtain with a given Boron-10 concentration. In the next section, an effort has also been made on developing transport models to investigate the issues of accurate modeling of control rods.

6. Evaluation of 3-D PBMR Transport Effects.

The failure of diffusion theory to model highly absorbing regions is well known and numerous methods have been developed to overcome it by using the so-called equivalent diffusion parameters. In the PBMR design, the positioning of these highly absorbing regions in the side reflector, where the leakage out of the core adds a directional dependence to the flux, further complicates the problem. One of these methods is the Method of Equivalent Cross Sections, (MECS) which was proposed by (Scherer, 1976 and Fen, 1992). The principle is to model the absorber and its environment in transport theory (S_N) and then extract cross sections and diffusion parameters from the transport solution that will represent the absorber region accurately in subsequent 3-D diffusion calculations. Another very simplified method available, called the Equivalent Boron Concentration (EBC), consists of adding a certain amount of boron absorber homogeneously into a "borated region" representing the control rod. The concentration of the boron is adjusted so that the control rod worth is conserved. The method assumes that the rod reactivity worth is known from experiment or other methods such as MECS.

In this work the 3D neutron transport S_N code TORT [7], was used with the cross sections generated with MICROX-2 to perform control rod worth calculations with control rods accurately and explicitly modeled in three-dimensions. The implemented approach was to first obtain the accurate control cross sections and to apply them in the neutronics code, while at the same time developing the best possible geometric representation of the control rod in TORT. The main objective of these studies was to obtain an optimum control rod representation in TORT, and use the differential control rod worth curve resulting from this configuration to adjust the 2-D DORT-TD control rod approximation so that accurate transient analysis can be performed with the currently developed coupled code DORT-TD/THERMIX. The first step was to evaluate the accuracy of the grey curtain representation of control rods by comparing it to MCNP results and then proceed to develop an explicit 3-D model in TORT and MCNP.

6. 1. Developed Core and Control Rod Models

In this study, three control rod models were developed and evaluated. The first one as mentioned above was the grey curtain representation. The grey curtain was used in DORT (r-z geometry) and also was used in TORT (r-θ-z geometry) with a dummy theta dimension. This exercise was meant to verify TORT, because in case of using the same cross sections and the dummy theta dimension, the TORT model is the same as the DORT model, hence one expects that the results obtained by the two codes should ideally be the same. This grey curtain model was also developed with MCNP, just for verification purposes. Secondly, an explicit model in MCNP was developed to represent the control rods explicitly i.e. not as a grey curtain. Finally a TORT model was developed and was made to be as close as possible to the explicit MCNP to accurately model the control rod configuration of the PBMR 268 MW design. Before proceeding to the models themselves, it is important to first discuss the PBMR control rod design.

The control rods in the PBMR are located in holes in the side reflector. These "sleeves" are made of graphite and the control rod is an annulus of Boron carbide within a cladding, as shown in Figure 11.

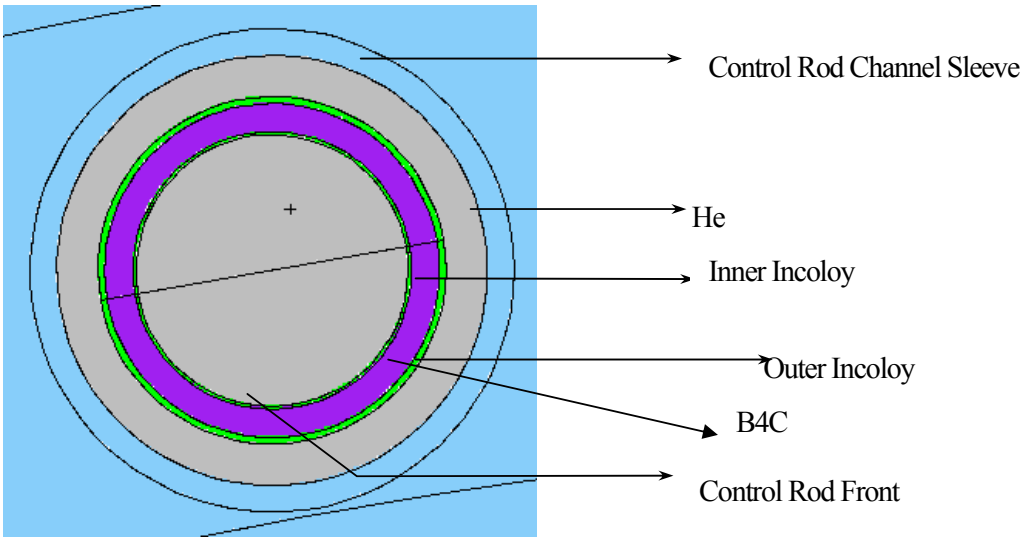

Figure 11: PBMR Control Rod Design

There are 18 control rods and 17 shut down rods filled with small absorber spheres called KLAKS. For purposes of this study, the shut down elements were not modeled as these are not used during normal operation. Inner radius of control rod channel sleeve is 6.5 cm and the outer radius is 7.3 cm. In this study, the control rod can be inserted as far as 850 cm, which is the height of the active core. In the actual PBMR design, control rods are divided into two sets, with 9 inserted from the bottom and 9 from the top, thereby creating a possibility of control rod overlap. For purposes of this work, all rods are assumed to be inserted from the top and no rod overlap is considered.

In both TORT and MCNP, the utilized design data was obtained from the PBMR Company in South Africa, and this is the same data the designers use for their models. From this data, the MCNP model was developed for Case N2 of the PBMR 268 MW benchmark problem as discussed in the introductory sections of this paper. Since this case requires cross sections generated at 900K and MCNP usually performs calculations at room temperatures, further cross section processing was performed with the NJOY code [8] in order to produce the cross section file xsdir for MCNP at 900K. As mentioned earlier, two MCNP models were developed, namely, MCNP-grey curtain and MCNP-explicit. These models are shown in Figures 12 and 13.

In developing the TORT model of the PBMR, BOT3P, the preprocessor (and postprocessor) of DORT and TORT was used. This approach was chosen because it would eliminate the possibility of geometrical errors in the model. With BOT3P, the user can actually visualize the geometry of the model and one of the salient features of this tool is that it can make the necessary adjustment in case of simple mistakes like overlaps or mesh size. It also has features that ensure that the volume of the model is preserved in case of some approximations due to small mesh size. The resulting TORT model is shown in Figure 14.

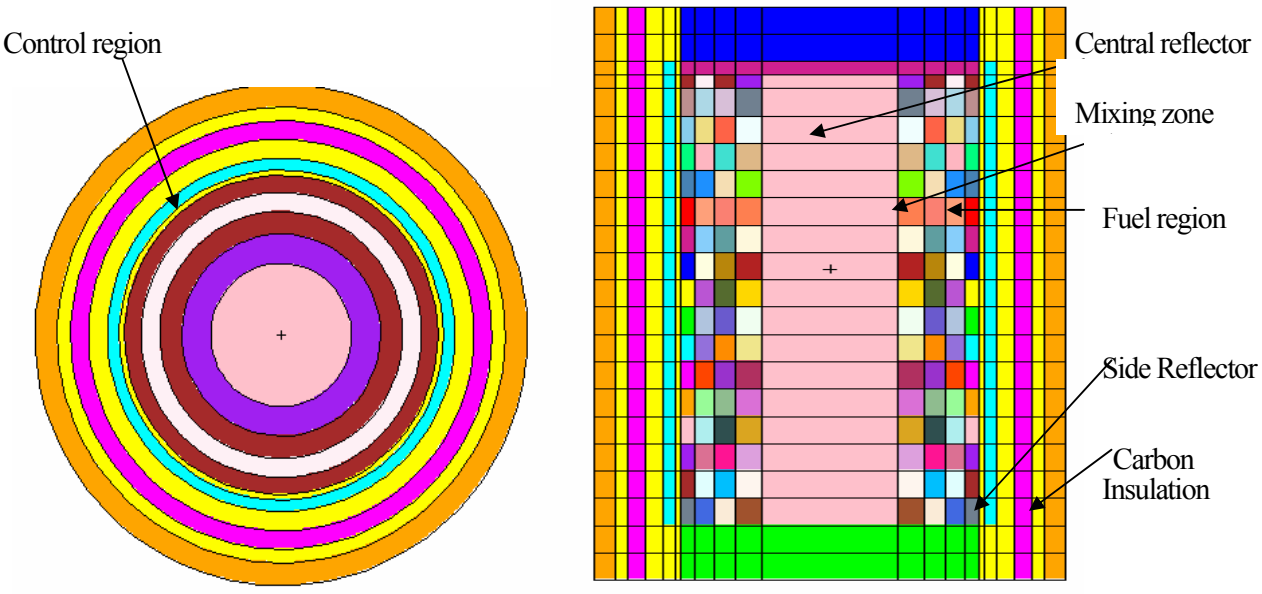

Figure 12: Radial and Axial View of the PBMR 268 MW MCNP Model with Grey Curtain CR

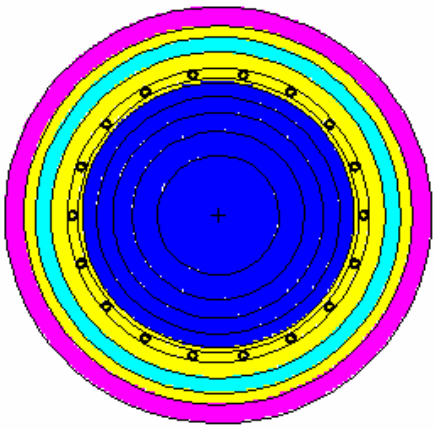

Figure 13: Top View of the PBMR 268 MW MCNP Model with Explicit CR Modeling

6.2 Control Rod Worth Calculations and Results.

With the developed models core calculations were performed with a view of computing control rod worths for each model. Firstly, it was important to verify that with TORT and DORT, using the same cross sections, a dummy theta dimension in TORT, and the grey curtain representation of the control region, the results will be the same as expected. Calculations were performed at various insertion depths of the grey curtain with steps of 100 cm. The obtained results are shown in Figure 15.

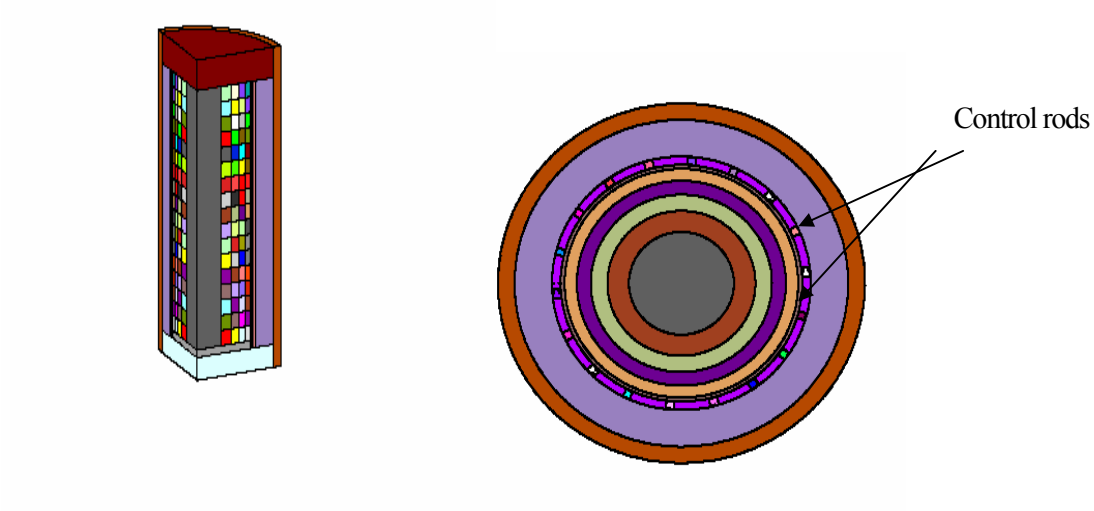

Figure 14: Radial and Axial View of the PBMR 268 MW TORT Model with Explicit CR Modeling

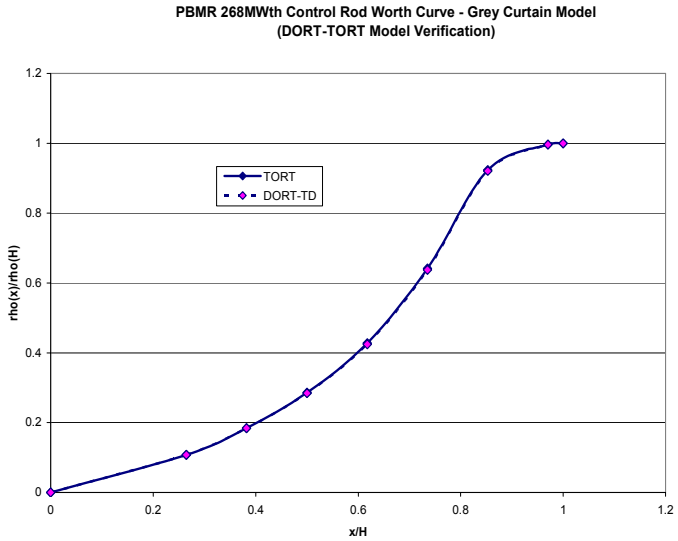

Figure 15: Integral Control Rod Worth as a Function of CR insertion

In Figure 15 the ratio of rod reactivity worth at a given insertion step to rod reactivity worth when rods are fully inserted is plotted against x/H where x is the insertion step or distance, and H is the height of the active core, in this case 850 cm. From the figure, it is clear that as expected, TORT in two dimensions completely reproduced the DORT results. The same calculations were performed with MCNP using the grey curtain representation of the control region. The results of MCNP were compared with those of DORT and TORT and as shown in Figure 16, other than the apparent shift in the integral control rod worth curve as the control rods are inserted deeper into the core, there is a reasonable agreement between the results.

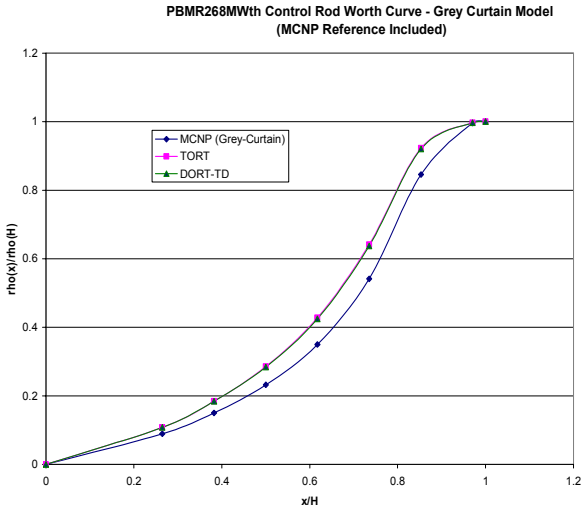

Figure 16: Integral Control Rod Worth as a Function of CR Insertion

The main objective of performing these calculations is to finally benchmark the DORT-TD code for PBMR and to later couple it with THERMIX-DIREKT. The coupled code will be used for transient analysis and one of the envisioned transient cases to be modeled with the coupled code is the rod ejection incident. It is therefore important that DORT-TD can model rod worth calculations accurately. In two-dimensions, the only feasible way to model control rods is by means of a grey curtain approximation. For this reason, rod worth calculations from DORT-TD are compared with the MCNP explicit model. Note that for all MCNP results, 50000 particles per generation were used with 1000 inactive cycles and 3000 active cycles for a total of 150 million particles. The MCNP eigenvalue results showed a standard deviation of 5 pcm while the power distribution results had a maximum standard deviation of 0.05%

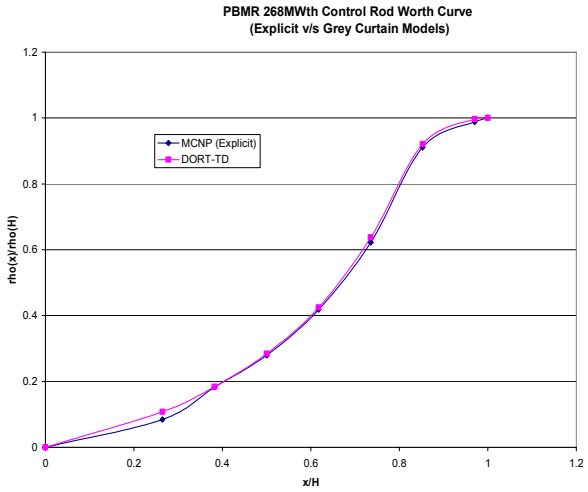

Figure 17: Integral Control Rod Worth as a Function of CR Insertion

It can be concluded from Figure 17, that the grey-curtain model in DORT-TD agrees well with the results of MCNP using explicit representation of control rods in the PBMR 268 MW design.

The results presented above have been obtained from a symmetric rod movement, i.e. it is assumed that the whole bank of control rods is moved. It is also important to model an asymmetric movement of control rods and to be able to do that, a three-dimensional deterministic model is necessary. The TORT model presented in Figure 14 was utilized for this purpose. Using the EBC method, calculations were initially performed with MCNP (explicit model) with all control rods inserted in the core and the resulting eigenvalue was noted. Subsequently, an iterative series of calculations was performed between MICROX, GIP and TORT, in order to find a k_{eff} value in TORT, which is reasonably close to the MCNP value. The Boron number density in MICROX was adjusted accordingly and cross sections were generated and arranged into a format readable by GIP. GIP was then used to process the cross sections into the FIDO format used by TORT and core calculations were then performed with TORT. This process was repeated until the target k_{eff} value was obtained with TORT. With the final cross sections obtained, the calculation is repeated with all rods withdrawn and the comparison between TORT and MCNP yielded a good agreement. Finally, a series of calculations with both TORT and MCNP was performed where, a single rod and subsequently a combination of rods in an asymmetric arrangement were inserted while the rest were fully withdrawn and the corresponding reactivity worth was calculated. The results from these calculations are summarized in Table 5 and Figure 18.

Table 5: Reactivity Worth of Combination of Control Rods

Combination	MCNP (dk/k)	TORT (dk/k)	% Difference
CR1+CR4+CR7	-0.02192	-0.02239	-2.16307
CR1+CR5+CR11	-0.02458	-0.02458	-0.0256
CR1+CR10	-0.01617	-0.0166	-2.6339
CR1+CR13+CR17	-0.02119	-0.02114	0.221495

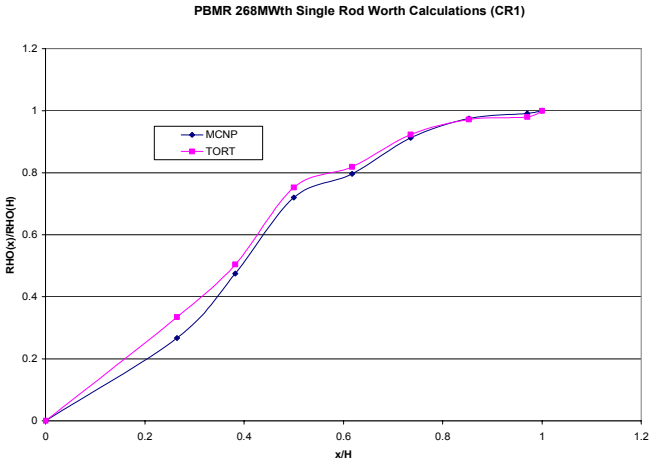

Figure 18: Integral Control Rod Worth as a Function of CR Insertion for CR1

7. Conclusions and Future Activities

The continuing growth in computational power and the need for sound physics models, especially for novel reactor concepts and designs such as the PBMR for which little intuitive experience exists, is continually placing the transport theory to the forefront of reactor analysis. In this paper, we have demonstrated the feasibility of this and the apparent benefits of choosing this route by using the

well-known DORT and TORT codes for PBMR applications. The deterministic codes were also verified with MCNP and excellent agreement was observed throughout. The developed models are important for benchmarking design codes used in new reactor concepts like the PBMR. The logical extension to this work is the utilization of transport theory based methods for transient analysis. Work is already ongoing to couple DORT-TD with THERMIX-DIREKT and subsequent testing of the coupled code with PBMR transient benchmarks that are also ongoing.

References

1) J.O. Johnson, "A users manual for Mash 1.0, a Monte Carlo Adjoint Shielding Code System (Contains the documentation for DORT), Oak Ridge National Laboratory Report ORNL/TM-11778, (1992)
2) S. Struth., "Direkt – A Computer Programme for non- steady, two-dimensional simulation of thermo-hydraulic transients," Kernforschunsanslage Jülich, JÜL-1702, March 1999
3) B. Tyobeka, K. Ivanov "Analysis of the PBMR-268 benchmark transient cases with the NEM-THERMIX coupled code" Transactions of the ANS Winter Meeting, November 2004, Washington DC, USA
4) Pautz, A. Birkhoffer, "Coupling of time-dependent neutron transport theory with the thermal hydraulics code ATHLET and Application to the Research Reactor FRM-II," Nucl. Sci. Eng. 145 pp 167-180, (2003)
5) F. Reitsma, B. Tyobeka, and K. Ivanov, "PBMR Steady-state Core Physics Benchmarks – Final Specification", PBMR Ltd./PSU, (2002).
6) D. Mathews, "An Improved Version of the MICROX-2 Code," Paul Scherrer Institute, Switzerland, PSI Bericht Nr. 97-11, (1997).
7) 7W. A. Rhoades and D. B. Simpson, "The TORT Three-Dimensional Discrete Ordinates Neutron/Photon Transport Code," ORNL/TM-13221 (1997)
8) R.E. MacFarlane and D.W. Muir, "The NJOY Nuclear Data Processing System", Version 91, LA-12740-M (1994)"